Effect of temperature oscillations on kinetic inductance and depairing in thin and narrow superconducting nanowire resonators

Jason P. Allmaras [1,*] Alexander G. Kozorezov [2] Marco Colangelo [3] Boris A. Korzh [1]
Matthew D. Shaw,[1] and Karl K. Berggren[3]

[1]*Jet Propulsion Laboratory, California Institute of Technology, Pasadena, California 91109, USA*
[2]*Department of Physics, Lancaster University, Lancaster LA1 4YB, United Kingdom*
[3]*Department of Electrical Engineering and Computer Science, Massachusetts Institute of Technology, Cambridge, Massachusetts 02138, USA*

(Received 2 December 2022; revised 20 February 2023; accepted 13 March 2023; published 30 March 2023)

Recent experiments have demonstrated a method for extracting the depairing current of nanowires fabricated from thin-film dirty superconductors using the AC response of DC-current biased resonators. While the existing theoretical model for understanding this response, developed by Clem and Kogan, provides agreement with Eilenberger-Usadel theory at low temperatures, there is a systematic and substantial deviation from theory at elevated temperatures. We propose that the DC bias in the presence of electromagnetic oscillations leads to Joule heating in the superconductor. This heating, combined with the strong electron-electron scattering in these heavily disordered materials, leads to oscillations in the effective temperature of the superconductor which alter the kinetic inductance. In this work, we derive the expression for the shift in kinetic inductance in the presence of a bias current and demonstrate that this model provides a significantly improved agreement between experiment and theory.

DOI: 10.1103/PhysRevB.107.104520

I. INTRODUCTION

The critical depairing current, I_d, and its dependence on temperature are important characteristics of superconducting nanowire single-photon detectors (SNSPD), but these properties are difficult to measure. Despite considerable effort, in real devices, the magnitude of the bias current above which the nanowire goes normal, named the switching current I_{sw}, is less than the critical depairing current, $I_{sw} \leqslant I_d$, with the typical ratio $0.5 \leqslant I_{sw}/I_d \leqslant 0.8$. This ratio is called the constriction factor, $C = I_{sw}/I_d$, and it is known to correlate with the variance of wire width connected with wire edge imperfections [1–3]. An experimental technique to determine the critical depairing current in thin superconducting nanowires was recently demonstrated by Frasca *et al.* [4]. This method measures the resonant frequency of superconducting half-wave coplanar waveguide resonator structures while carrying a finite DC bias current in order to extract the shift in kinetic inductance as a function of bias current from no bias current up to the switching current. To extract the depairing current, the experimental data is fit according to the theoretical calculation of the kinetic inductance for the response to a small alternating current under different bias and temperature conditions. The theoretical dependence calculated by Clem and Kogan (CK) [5] based on the solution of the Eilenberger-Usadel equations for the two asymptotic limits of either fast relaxation/slow experiment or slow relaxation/fast experiment is then used for fitting the experimental data. For both of these asymptotic limits, the depairing current is the single free fitting parameter.

The validity range for the above-mentioned asymptotic models remains somewhat imprecise. The fast relaxation model of CK is valid provided that the slowest of the relevant relaxation processes is faster than the frequency of alternating electric field, $\omega \ll \min\{1/\tau_i\}$ (slow experiment), where the index i labels the relevant internal relaxation times [6–8]. Conversely, for the slow relaxation model the validity criterion is $\omega \gg \max\{1/\tau_i\}$ (fast experiment). In the intermediate frequency range, there are a number of possible responses depending on the relationships between the various $1/\tau_i$ and ω, but the overall range of frequencies for the region between the fast and slow relaxation regimes is expected to be relatively small. Based on the solution of the simplified time-dependent Ginzburg-Landau (TDGL) equations with the single relaxation time τ_s rather than several intrinsic relaxation times, Clem and Kogan derived the expression for the response in the intermediate regime, correctly reproducing the results of both models within their validity ranges, and also bridging across these limits via smoothly varying interpolation.

After the original experimental work [4], we subsequently reanalyzed the original data and additional data collected on WSi samples [1] and found that the fitting based on the CK model extracts the correct critical depairing current only in the low temperature limit $T \to 0$. At elevated temperatures ($T \gtrsim 0.3T_c$, with T_c being the critical temperature), the temperature dependence of the experimentally extracted $I_d(T)$ based on the CK model exhibits a systematic and substantial deviation from the theoretical temperature dependence calculated by Kupriyanov and Lukichev [9]. The reason for this deviation, which was observed in all studied

*allmaras@jpl.caltech.edu

samples of NbN and WSi nanowires, has not been previously explained.

The direct measurement of the critical depairing current is a crucial tool for superconducting nanowire characterization both for understanding fabrication quality [1] and for making quantitative comparisons between the SNSPD detection mechanism theory [10–12] and experiment [13]. Therefore, it is important to understand the reasons for the apparent failure of the CK model at elevated temperatures. The objective of this paper is to analyze this discrepancy between theory and experiment in detail. In Sec. II we review the existing CK theory and demonstrate its failure to generate agreement between experiment and theory over a wide temperature range. We subsequently show that normalization of the data from all samples leads to a universal form of this error and basic extensions of the CK model are incapable of removing the discrepancy between theory and experiment. We hypothesize that in the experimental regimes studied to date [1,4], Joule heating occurs due to the interaction of the finite resistive component of the impedance of the nanowire with the driving alternating field, and that the dynamics of this energy exchange are important to understanding the response of the superconducting system. In Sec. III we derive a generalized CK fast relaxation model which includes the effect of temperature oscillations in the small signal limit. Section IV contains a discussion of the modified CK-T-oscillations model and a detailed comparison of experiment with theory, showing a substantial improvement in the agreement between experiment and theory.

II. KINETIC IMPEDANCE AND DEPAIRING IN THIN SUPERCONDUCTING NANOWIRES IN THE ABSENCE OF TEMPERATURE OSCILLATIONS

The general result [5] for the DC-current-dependent kinetic inductance, $\mathcal{L}_k(q,T)$, can be written in the form

$$\frac{\mathcal{L}_k(q,T)}{\mathcal{L}_k(0,T)} = \frac{1}{\omega\mu_0\lambda_0^2(T)}\mathrm{Im}(\mathcal{Z}_{ks}). \tag{1}$$

Here $\mathcal{Z}_{ks}$ is complex kinetic impedivity, $q = 2mv_s/\hbar$ is the superfluid momentum, and ω, μ_0, and $\lambda_0(T)$ are the frequency of the alternating electric field, magnetic permeability of free space, and material weak field London magnetic penetration depth at zero current, respectively. In the definition of superfluid momentum, m is the electron mass and v_s is the superfluid velocity.

Model of Clem and Kogan

Using simplified TDGL equations, Clem and Kogan derive the expression for the complex kinetic impedivity in the Ginzburg-Landau (GL) limit in the form

$$\mathcal{Z}_{ks}^{GL} = i\omega\mu_0\lambda_0^2(T)\frac{F_s^{GL} + F_f^{GL} i\omega\tau_{\mathrm{eff}}}{1 + i\omega\tau_{\mathrm{eff}}}, \tag{2}$$

where $\tau_{\mathrm{eff}} = \frac{1}{2}F_s^{GL}\tau_s$,

$$\tau_s = \frac{\pi\hbar}{8k_B(T_c - T)} \tag{3}$$

is the order parameter relaxation time, $\hbar$ is the reduced Planck constant, k_B is the Boltzmann constant, and T_c is the critical temperature. The functions F_s^{GL} and F_f^{GL} are the GL limits of the more general expressions F_s and F_f, defining the kinetic inductivity in the limits of slow and fast experiment as $\frac{\mathcal{L}_k(q,T)}{\mathcal{L}_k(0,T)} = F_{\{s,f\}}(\frac{|I_b|}{I_d(T)})$, where I_b is the bias current. The general expressions are

$$F_s\left(\frac{|I_b|}{I_d(T)}\right) = \lambda_0^{-2}(T)\left[\frac{d}{dq}\left(\frac{q}{\lambda_q^2(T)}\right)\right]^{-1}, \tag{4}$$

$$F_f\left(\frac{|\bar{I}_b|}{I_d(T)}\right) = \frac{n_{s0}(T)}{n_{s\bar{q}}(T)}, \tag{5}$$

where $n_{s\bar{q}}(T)$ is the superfluid density at q and T where the bar denotes time averaging. The subscript q in $\lambda_q(T)$ indicates the dependence on the penetration depth on q. These functions of q and T were found [5] by solving the Usadel equations numerically. Their GL limits were derived analytically [5]. The corresponding expressions are

$$F_s^{GL}(x) = \frac{1}{2\cos[2\phi(x)/3] - 1}, \tag{6}$$

$$F_f^{GL}(x) = \frac{3}{1 + 2\cos[2\phi(x)/3]}, \tag{7}$$

where $\phi(x) = \arcsin x$. The simple expression (2) derived under the usual constraints of the GL approach describes both the low and high microwave frequency limits (slow and fast experiments, respectively) and it might be also useful in providing sensible interpolation between the two limits $\omega\tau_{\mathrm{eff}} \ll 1$ and $\omega\tau_{\mathrm{eff}} \gg 1$. Moreover, because a direct comparison between the functions F_s, F_f and their GL counterparts F_s^{GL}, F_f^{GL} reveals that their difference over the whole range of temperatures and currents up to I_{sw} is small, typically less than 2%, we expect that it is not unreasonable to keep the result (2) replacing F_s^{GL}, F_f^{GL} by F_s, F_f as sensible interpolation for the whole range of temperatures as suggested by CK [5], leading to

$$\mathcal{Z}_{ks} = i\omega\mu_0\lambda_0^2(T)\frac{F_s + F_f i\omega\tau_{\mathrm{eff}}}{1 + i\omega\tau_{\mathrm{eff}}}. \tag{8}$$

To compare theory and experiment throughout this work, we use the data collected by Frasca *et al.* [4] and Colangelo *et al.* [1]. To apply the CK model, we start by estimating the magnitude of the parameter $\omega\tau_{\mathrm{eff}}$. Taking a microwave frequency of 2 GHz and T_c=8.65 K for NbN wires and 2 K $< T_c <$ 3.5 K for WSi wires we arrive at characteristic values for this parameter in the range of 0.005–0.015 for the NbN from Frasca *et al.*, 0.01–0.03 for the WSi with $T_c = 3.5$ K from Frasca *et al.*, and 0.05–0.1 for the WSi with $T_c = 2$ K from Colangelo *et al.* Therefore, for all but the WSi wires with T_c=2 K the fast relaxation/slow experiment CK model can be used with high accuracy. This is consistent with a previous analysis [4] where direct comparison reveals that a much better fit of $\frac{\mathcal{L}_k(q,T)}{\mathcal{L}_k(0,T)}$ is achieved with the fast relaxation model. Figure 1 illustrates the comparison between theory and experiment of the temperature-dependent depairing current extracted from the CK models for NbN and WSi nanowires. The T dependence shown by the blue curves was derived from

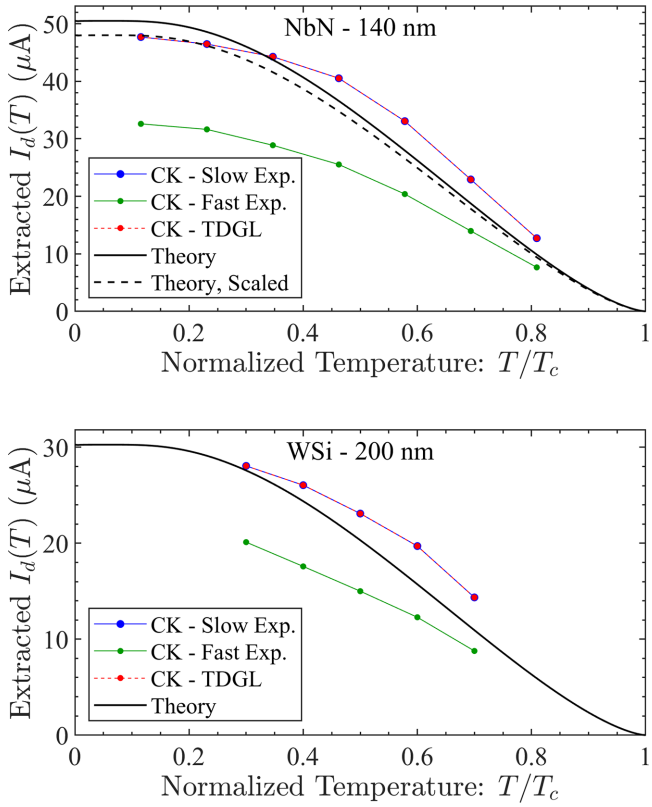

FIG. 1. Critical depairing current derived from the CK slow experiment/fast relaxation model (blue), CK fast experiment/slow relaxation model (green), and CK simplified TDGL model (red) for a 140 nm NbN wire [4] and 200-nm-wide WSi wire [4]. The simplified TDGL model coincides with the fast relaxation model. The expectation based on theory and material parameters [9] is shown in black, indicating a significant deviation from the expected fast relaxation model results. The dashed black line in the NbN plot shows the same theoretical temperature dependence but with $I_d(0)$ scaled to 48.0 μA to match the experimental data.

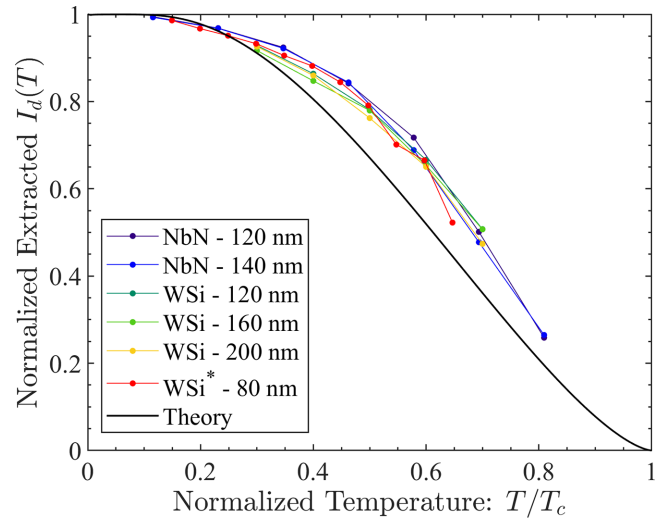

FIG. 2. Normalized critical depairing current derived from the CK fast relaxation model vs temperature for 120-nm- (39.0 μA) and 140-nm- (48.0 μA) wide NbN wires [4], 120-nm- (16.8 μA), 160-nm- (23.7 μA), and 200-nm- (30.3 μA) wide WSi wires [4], and a lower T_c 80-nm (3.62 μA) WSi* wire [1]. The asterisk is used to indicate the lower T_c WSi stoichiometry. The currents listed in parentheses by each nanowire width indicate the value of $I_d(0)$ used for normalization.

experimental data using the CK fast relaxation/slow experiment model, the green curve shows the T dependence derived from the CK slow relaxation/fast experiment model, and the red curve shows the CK TDGL-based model. As expected, the TDGL-based model generates an $I_d(T)$ curve which nearly coincides with the fast relaxation/slow experiment result for both NbN and WSi wires. The solid black line indicates the theoretical curve [9] based on the numerical solution of the Usadel equations and the measured material parameters for each of the samples. A substantial discrepancy between the CK-derived and theoretical $I_d(T)$ is evident.

There are two aspects of this deviation which should be considered separately. First is the deviation between the zero temperature depairing current

$$I_d(0) = 1.491eN(0)[\Delta(0)]^{3/2}\sqrt{D/\hbar}\,wd \tag{9}$$

and the value extrapolated to zero temperature from the experimental data and the CK model. In this expression, e is the elementary charge, $N(0) = (2e^2DR_\square d)^{-1}$ is the single-spin electron density of states at the Fermi level in the normal state, $\Delta(0) = 1.764k_BT_c$ is the magnitude of the superconducting gap at zero temperature, D is the diffusion coefficient, $R_\square$ is the sheet resistance, w is the width, and d is the thickness. The deviation between theory and experiment at zero temperature is particularly evident for the NbN sample at approximately 5%, but it should be noted that the diffusion coefficient used in that calculation was from the literature and not directly measured for that sample and could be a substantial source of error.

The second deviation, and the one which is the focus of this work, is in the temperature dependence of $I_d(T)$. While $I_d(0)$ is strongly dependent on the particular material parameters of the device, when normalized as $I_d(T)/I_d(0)$ and T/T_c, the theoretical dependence has a universal form [9]. Therefore, while deviations in $I_d(0)$ can easily be understood to be consistent with theory under the assumption of imperfect or incomplete measurement of material parameters, the deviation between the temperature dependence of theory and experiment presents a serious problem for the CK model used in the experimental fitting procedure. To illustrate this, Fig. 2 shows the difference between theory and the $I_d(T)$ derived from measurements using the CK fast relaxation model for several NbN and WSi nanowires of different widths, all falling within the validity range of the fast relaxation model, in dimensionless units. The normalization of $I_d(T)$ was performed by extrapolating the experimentally extracted I_d to zero temperature to determine $I_d(0)$ rather than using material parameters and Eq. (9). All curves fall into a universal form with a substantial deviation from theory. This is the problem we seek to address in this work.

It is natural to first explore simple modifications to the CK model in an attempt to reconcile this discrepancy. The CK approach uses the standard TDGL timescale for interpolating between the fast and slow relaxation regimes. Extending

this to the generalized TDGL approach [14,15] which modifies the timescale of relaxation does not improve the fitting for realistic values of the scattering times as shown in Appendix A. Another modification is to study the effect of the presence of additional pair breakers in the material using the Abrikosov-Gor'kov theory [16] within the CK formalism, but this approach also fails to reconcile theory with experiment as demonstrated in Appendix B. Given the failure of these two approaches, it is clear that a more fundamental change to the model formulation is required.

III. KINETIC IMPEDANCE AND DEPAIRING IN THIN SUPERCONDUCTING NANOWIRES: EFFECT OF TEMPERATURE OSCILLATIONS

In this section we generalize the fast relaxation theory of Clem and Kogan by incorporating the effect of thermal oscillations induced in a current-carrying superconductor by an alternating electric field through the use of the two-temperature model. The use of temperature oscillations explicitly assumes that the electron-electron interactions occur much faster than the driving frequency $\omega\tau_{ee} \ll 1$ in order for the excited quasiparticle distribution to be described by a thermalized distribution, where τ_{ee} is the electron-electron relaxation time. Our estimates under the conditions discussed in the Supplemental Material [17] indicate that $\omega\tau_{ee} \leqslant 1$ for $T \gtrsim 0.3 - 0.35T_c$ for the materials investigated in Refs. [1,4] which is the precisely the regime where there is a significant deviation in the temperature dependence of $I_d(T)$ of theory compared to experiment. While the formal requirement of $\omega\tau_{ee} \ll 1$ is not strictly satisfied for the full temperature range of interest, the estimate that $\omega\tau_{ee} \leqslant 1$ indicates that at least partial thermalization is expected to occur. Given the dramatic simplification of the problem and the at least partial justification of the approach, we proceed with using the two-temperature model. Furthermore, our approach assumes that the oscillation frequency is slow with respect to the relevant timescale of superconductor relaxation. A better approximation is to use the assumption of quasiequilibrated electrons and nonequilibrium phonons; however, we expect it to provide only a marginal improvement for the frequency range and material parameters under consideration. Beyond these limits, the more complicated approach of using the full nonequilibrium response of the electrons and phonons is needed.

In the limit of a small oscillating bias current, the temperature oscillations are assumed to have a form

$$T_e(t) = T_{e0} + \delta T_e e^{i\omega t}, \tag{10}$$

$$T_{ph}(t) = T_{ph0} + \delta T_{ph} e^{i\omega t}, \tag{11}$$

where $T_{e,ph}(t)$ is the time-dependent temperature, $T_{e0,ph0}$ is a constant baseline temperature, and $\delta T_{e,ph}$ is the complex amplitude of the oscillating contribution of the temperature for the electron and phonon systems, respectively. In the energy balance equations, we can neglect the spatial derivatives (thermal conductivity terms) because the length scale of the corresponding temperature gradients is on the order of the RF wavelength, which is several hundred micrometers in these structures. This leads to the equations

$$\frac{\partial E_e(q,T_e)}{\partial t} = \frac{E_0}{\gamma}\int_0^\infty d\epsilon\,\epsilon^3\nu(\epsilon)\left[N_\epsilon^0(T_{ph}) - N_\epsilon^0(T_e)\right] + \vec{j}(t)\vec{E}(t) \tag{12}$$

and

$$\frac{\partial T_{ph}}{\partial t} = -\frac{T_{ph}^4 - T_{\rm sub}^4}{4\tau_{\rm esc}T_{ph}^3} - \frac{15}{4\pi^4}\frac{T_c^4}{T_{ph}^3}\int_0^\infty d\epsilon\,\epsilon^3\nu(\epsilon) \times \left[N_\epsilon^0(T_{ph}) - N_\epsilon^0(T_e)\right]. \tag{13}$$

Here $E_e(q,T_e)$ is the electronic energy density depending on both supermomentum and temperature, $E_0 = 4N(0)k_B^2T_c^2$, N_ϵ^0 is the Planck distribution function, $\nu(\epsilon)$ is the phonon-electron scattering rate, $\vec{j}(t)$ is the current density, $\vec{E}(t)$ is the electric field, $\tau_{\rm esc}$ is the phonon escape time, $T_{\rm sub}$ is the substrate (bath) temperature, and the parameter $\gamma = (\pi^4/15)C_e(T_c)/C_{ph}(T_c)$ is proportional to the ratio of the electron and phonon heat capacities [$C_e(T)$ and $C_{ph}(T)$, respectively] at T_c. For convenience in subsequent transformations, in the energy balance Eqs. (12) and (13) the terms describing the energy exchange between electrons and phonons are written (with the appropriate signs) in the form of energy transfer rates from phonons to quasiparticles.

In the limit of small temperature oscillations, keeping terms to first order in δT_e and δT_{ph}, and taking $T_{e0} = T_{ph0} = T_{\rm sub} = T$ because there is not sufficient AC Joule heating to raise the average temperature of the electron or phonon systems, we arrive at the temperature variation equations

$$\frac{\partial E_e(q,T)}{\partial T}i\omega\delta T_e e^{i\omega t} + \frac{\partial E_e(q,T)}{\partial q}\frac{dq}{dt} = \vec{j}(t)\vec{E}(t) + \frac{E_0}{\gamma}\int_0^\infty d\epsilon\,\epsilon^3\nu(\epsilon)\frac{\partial N_\epsilon^0}{\partial T}(\delta T_{ph} - \delta T_e)e^{i\omega t} \tag{14}$$

and

$$\left(i\omega + \frac{1}{\tau_{\rm esc}} + \frac{1}{\tau_2}\right)\delta T_{ph} = \frac{1}{\tau_2}\delta T_e \tag{15}$$

for the electron and phonon systems, respectively. Here we introduce the second timescale

$$\frac{1}{\tau_2} \equiv \frac{15}{4\pi^4}\frac{T_c^4}{T^3}\int_0^\infty d\epsilon\,\epsilon^3\nu(\epsilon)\frac{\partial N_\epsilon^0}{\partial T} \tag{16}$$

to simplify the phonon equation. The expression for $\nu(\epsilon)$ can be derived from the phonon-electron collision integral to describe the energy exchange between the two systems within the two-temperature model. We obtain

$$\nu(\epsilon) = \frac{\gamma}{\tau_0 k_B T_c}\frac{1}{N_\epsilon^0}\left\{\int_{\epsilon_g}^{\epsilon-\epsilon_g} d\epsilon_1 M(\epsilon_1, -(\epsilon-\epsilon_1))n_{\epsilon_1}^0 n_{\epsilon-\epsilon_1}^0 + 2\int_{\epsilon_g}^\infty d\epsilon_1 M(\epsilon_1, \epsilon+\epsilon_1)\left(1-n_{\epsilon_1}^0\right)n_{\epsilon+\epsilon_1}^0\right\}, \tag{17}$$

where τ_0 is the characteristic electron-phonon interaction time [6] and $n_{\epsilon_i}^0$ is the equilibrium Fermi distribution function. The expression for the function M is $M(\epsilon, \pm\epsilon_1) = N_1(\epsilon)N_1(\epsilon_1) \mp R_2(\epsilon)R_2(\epsilon_1)$. For a current-carrying superconductor, N_1 and

R_2 are found through the numerical solution of the Usadel equations. For a normal metal, taking $\epsilon_g = 0$, $M(\epsilon, \epsilon_1) = 1$, performing the integration in (17) and then in (16), we obtain $\tau_2 \equiv \frac{\tau_0 \pi^4}{450\gamma\zeta(5)} \frac{T_c}{T}$.

Finally, we write the phonon temperature modulation as

$$\delta T_{ph} = \frac{\frac{1}{\tau_2}}{\left(i\omega + \frac{1}{\tau_{\rm esc}} + \frac{1}{\tau_2}\right)} \delta T_e. \tag{18}$$

We can substitute (18) back into the electron temperature equation (14) to obtain an expression for the electron temperature oscillations. Rearranging this in terms of the time derivative of T_e through $\frac{dT_e}{dt} = i\omega \delta T_e e^{i\omega t}$, we arrive at

$$\frac{dT_e/T_c}{dt} = i\omega \frac{\vec{j}(t)\vec{E}(t) - \frac{\partial E_e(q,T)}{\partial q}\frac{dq}{dt}}{\left(\frac{\partial E_e(q,T)}{\partial (T/T_c)} i\omega + \frac{4\pi^4}{15\gamma}\left(\frac{T}{T_c}\right)^3 \frac{E_0}{\tau_2} \frac{i\omega + \frac{1}{\tau_{\rm esc}}}{i\omega + \frac{1}{\tau_{\rm esc}} + \frac{1}{\tau_2}}\right)}. \tag{19}$$

To continue, we must define the form of oscillations in the electric field $\vec{E}(t)$. For simplicity, we consider the one-dimensional case as done by Clem and Kogan and neglect the vector notation for superfluid momentum q, electric field E, and current j. We start by defining the current according to

$$j_s(t) = j_{s0} + j_{s1}(t) = j_{s0} + j'_{s1} e^{i\omega t}, \tag{20}$$

where j_{s0} is the DC supercurrent, $j_{s1}(t)$ is the oscillating part of the supercurrent, and j'_{s1} is the amplitude of current oscillations. Following the definition

$$E = \mathcal{Z}_{ks} j_{s1} = (\mathcal{R}_{ks} + i\omega \mathcal{L}_k) j_{s1}, \tag{21}$$

where $\mathcal{R}_{ks}$ is the resistivity, we rewrite the kinetic inductance (1) in the form

$$\mathcal{L}_k = \frac{1}{\omega} \mathrm{Im}\left(\frac{E}{j_{s1}}\right). \tag{22}$$

For a one-dimensional wire carrying uniform current, we have [5]

$$E = -\frac{\phi_0}{2\pi} \frac{dq}{dt} \tag{23}$$

and using the sinusoidal variation of j_{s1}

$$j_{s1} = \frac{1}{i\omega} \frac{dj_{sq}[T(t)]}{dt} \tag{24}$$

with the notation of CK [5] where the subscript to j_{sq} denotes the supercurrent for a given value of q, we arrive at the following definition of the kinetic inductance:

$$\mathcal{L}_k = \frac{1}{\omega} \mathrm{Im}\left(\frac{-\frac{\phi_0}{2\pi}\frac{dq}{dt}}{\frac{1}{i\omega}\frac{dj_{sq}[T(t)]}{dt}}\right) = -\frac{\phi_0}{2\pi} \mathrm{Re}\left(\frac{\frac{dq}{dt}}{\frac{dj_{sq}[T(t)]}{dt}}\right), \tag{25}$$

where ϕ_0 is the flux quantum. If we expand the time derivative of the supercurrent, we have

$$\frac{dj_{sq}[T(t)]}{dt} = \frac{\partial j_{sq}(T)}{\partial q}\frac{dq}{dt} + \frac{\partial j_{sq}(T)}{\partial T}\frac{dT}{dt}. \tag{26}$$

The definition of the supercurrent

$$j_{sq}(T) = -\frac{\phi_0}{2\pi}\frac{q}{\mu_0 \lambda_q^2(T)} = -\frac{\phi_0}{2\pi}\frac{q}{\mu_0\lambda_0^2(0)}\frac{n_{sq}(T)}{n_{s0}(0)} \tag{27}$$

allows us to rewrite the derivative terms as

$$\frac{\partial}{\partial q} j_{sq}(T) = -\frac{\phi_0}{2\pi}\frac{1}{\mu_0\lambda_0^2(0)}\frac{\partial}{\partial q}\left[\frac{q\, n_{sq}(T)}{n_{s0}(0)}\right] \tag{28}$$

and

$$\frac{\partial}{\partial T} j_{sq}(T) = -\frac{\phi_0}{2\pi}\frac{q}{\mu_0\lambda_0^2(0)}\frac{\partial}{\partial T}\left[\frac{n_{sq}(T)}{n_{s0}(0)}\right]. \tag{29}$$

Introducing these into the definition of the kinetic inductance, we get

$$\frac{\mathcal{L}_k(q,T)}{\mathcal{L}_k(0,0)} = \mathrm{Re}\left(\frac{1}{\frac{\partial}{\partial q}\left[\frac{q\, n_{sq}(T)}{n_{s0}(0)}\right] + q\frac{\partial}{\partial T}\left[\frac{n_{sq}(T)}{n_{s0}(0)}\right]\frac{dT}{dt}/\frac{dq}{dt}}\right). \tag{30}$$

In the absence of temperature oscillations, the second term in the denominator of (30) goes to zero and the result converges to the CK expression for the fast relaxation model (4). We now introduce dimensionless units as indicated by a tilde: temperature in units of T_c, superfluid velocity in units $q_m(0) = \xi^{-1}(0)$, where $\xi(0)$ is the coherence length at $T = 0$, supercurrent density in units of the theoretical depairing current density $j_d(0)$ at $T = 0$ (9), and electronic energy density in units of E_0. Using the expression for electron temperature oscillations (19) for the temperature oscillation term, substituting (23) into Joule heat term, and noting that the temperature values for the non-time-dependent terms refer to the substrate temperature $\tilde{T} = \tilde{T}_{\rm sub}$, we finally arrive at

$$\frac{\mathcal{L}_k(\tilde{q},\tilde{T})}{\mathcal{L}_k(0,0)} = \mathrm{Re}\left(\frac{1}{\frac{\partial}{\partial\tilde{q}}\left[\frac{\tilde{q}\, n_{sq}(\tilde{T})}{n_{s0}(0)}\right] + \tilde{q}\frac{\partial}{\partial\tilde{T}}\left[\frac{n_{sq}(\tilde{T})}{n_{s0}(0)}\right]\frac{0.5799|\tilde{j}_{sq}(\tilde{T})| - \frac{\partial\tilde{E}_e(\tilde{q},\tilde{T})}{\partial\tilde{q}}}{\left(\frac{\partial\tilde{E}_e(\tilde{T},\tilde{q})}{\partial\tilde{T}} + \frac{4\pi^4}{15\gamma}\tilde{T}^3\frac{1}{i\omega\tau_2}\frac{\left(1+\frac{1}{i\omega\tau_{\rm esc}}\right)}{\left(1+\frac{1}{i\omega\tau_{\rm esc}}+\frac{1}{i\omega\tau_2}\right)}\right)}}\right), \tag{31}$$

where we use the convention $\tilde{q} \geqslant 0$ and include the absolute value of $\tilde{j}_{sq}(\tilde{T})$ to ensure the correct sign of that term.

IV. DISCUSSION

The derivation of our final result (31) appears to be a natural extension of the Clem and Kogan theory [5] in the limit where the superconductor remains in an equilibrium state (fast relaxation/slow experiment) at all times. The only essential assumption made so far was the incorporation of small temperature oscillations occurring due to Joule heating by an alternating electric field. Such oscillations occur naturally if the period of the alternating field is slow in comparison with the characteristic inelastic scattering time of the

electronic system. The possibility for this to happen on the timescale of single scattering events with small energy transfer in the case of quasielastic scattering is demonstrated in the Supplemental Material [17] for a normal disordered metal provided that the nonequilibrium state is induced by a spatially homogeneous low-frequency electric field. It is sensible to assume that this is also true for quasiparticle equilibration in a disordered superconductor. The linear response regime corresponds to the situation where the amplitude of the mean energy/temperature oscillations is small relative to equilibrium temperature $k_B T$. Therefore, in the small signal limit, the number of available thermally excited quasiparticles within a given spectral region exceeds the number of nonequilibrium excitations.

A. Comparison with experiment

Use of the temperature oscillation enhanced formulation of the kinetic inductance (31) to interpret experimental results is only justified when the experimental data is measured in the small-signal limit. In both experiments, the AC driving excitations were at the nanoampere level, which was verified not to suppress the switching current of the devices. Furthermore, the experiments of Frasca *et al.* [4] demonstrated that the measured resonant frequencies of the devices were insensitive to further reduction of the driving excitation. This is consistent with our expectation based on the linear response analysis used to derive (31) where the result is independent of the amplitude of the driving AC signal.

Using the enhanced formulation for the kinetic inductance (31), we can compare the temperature dependence of the experimentally extracted depairing current to theory. For all of our fits, we numerically calculate the electron-phonon scattering rate $\nu(\epsilon)$ for a superconductor based on Eq. (17) rather than use the simple analytical form for a normal metal. As with the standard CK model fitting procedure, I_d is the only free parameter used when fitting the experimental shift in kinetic inductance with bias current. For the NbN samples of [4], we use the material parameters $T_c = 8.65\,\mathrm{K}$, $\tau_{\mathrm{esc}} = 20\,\mathrm{ps}$, $\gamma = 20$, and $\tau_0 = 1.8\,\mathrm{ns}$. For the WSi samples of [4], we use the material parameters $T_c = 3.5\,\mathrm{K}$, $\tau_{\mathrm{esc}} = 50\,\mathrm{ps}$, $\gamma = 60$, and $\tau_0 = 9.1\,\mathrm{ns}$. Finally, for the MIR optimized WSi material of [1], we use $T_c = 2.01\,\mathrm{K}$, $\tau_{\mathrm{esc}} = 50\,\mathrm{ps}$, $\gamma = 182$, and $\tau_0 = 48\,\mathrm{ns}$. For both sets of experiments, the superconductors were deposited on SiO_2, which enters the model through the estimated phonon escape time.

The extracted depairing current for these different materials is shown in normalized units as depairing current vs temperature in Fig. 3. Normalization was performed by using the same $I_d(0)$ values as used in Fig. 2. When compared to Fig. 2, it is clear that the incorporation of temperature oscillations improves the quality of the fitting for all of the devices. In particular, the deviation between theory and experiment in the region $T > 0.3T_c$ is substantially reduced. As $T \to 0$, there is minimal change to the extracted depairing current based on the shift in kinetic inductance with bias current.

Our refined theory's impact on the extracted depairing current directly influences the constriction factor extracted using this method. Previous estimates of the depairing current using the CK fast relaxation model at elevated temperatures are systematically larger than the expected value of $I_d(T)$ based on theory and our refined model. This leads to underestimating the constriction factor and calculating the wrong temperature dependence, which makes the experimentally extracted reduction in constriction factor with increasing temperature appear more pronounced than it is. This is demonstrated in Fig. 4 where we plot the constriction factor extracted using the CK fast relaxation model compared to the constriction factor extracted using our refined model for a selection of samples from Refs. [1,4]. The correct measurement of the temperature dependence of the constriction factor and switching current is especially important for providing a means of testing models describing the switching of current-carrying superconducting nanowires to the normal state.

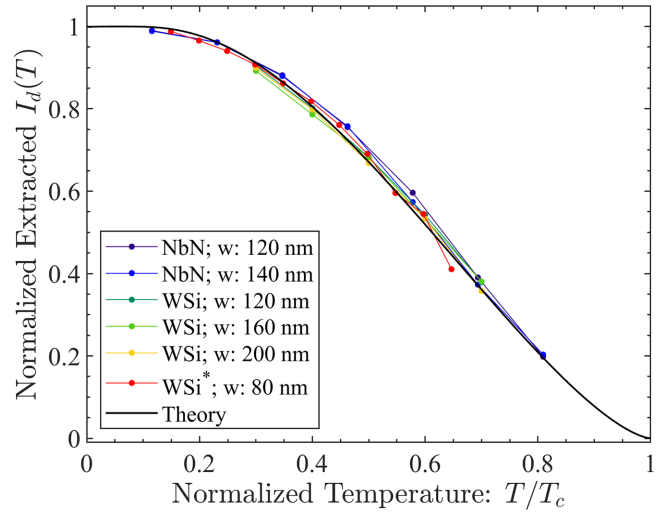

FIG. 3. Comparison of the extracted $I_d(T)$ using the temperature oscillation enhanced CK fast relaxation model for the NbN and WSi results of Frasca *et al.* [4] and the 80-nm-wide WSi* of Colangelo *et al.* [1] with the predictions of theory (black). Compared to the results of the standard CK fast relaxation model shown in Fig. 2, there is a significant improvement in the agreement between theory and experiment. The normalization factor $I_d(0)$ was the same as used in Fig. 2 for all of the devices.

Measurements of the critical depairing current for wires of different widths fabricated from the same material with the same processing quality is also believed to provide important information about the properties of the edges of the nanowires. Plotting I_d vs wire width for different bath temperatures $0 \leqslant T/T_c \leqslant 1$ reveals an offset width in the extrapolated zero current intercept of the width vs I_d curve [1,4]. The presence of an offset is qualitatively consistent with a lateral N-S-N or S-S′-S proximity effect resulting in the active area of the nanowire being smaller than the true wire width as discussed in Refs. [18,19]. However, this interpretation is potentially prone to error for the same reason as the temperature dependence of the constriction factor deduced from the CK model. By accounting for temperature oscillations while processing the experimental data both in [4] and [1], the derived $I_d(T)$ shifts closer to the theoretical curve, but the impact on the extracted offset is actually minimal because all of the curves used to generate the linear fit shift in a similar way at a given temperature (see Supplemental Material [17]). As fu-

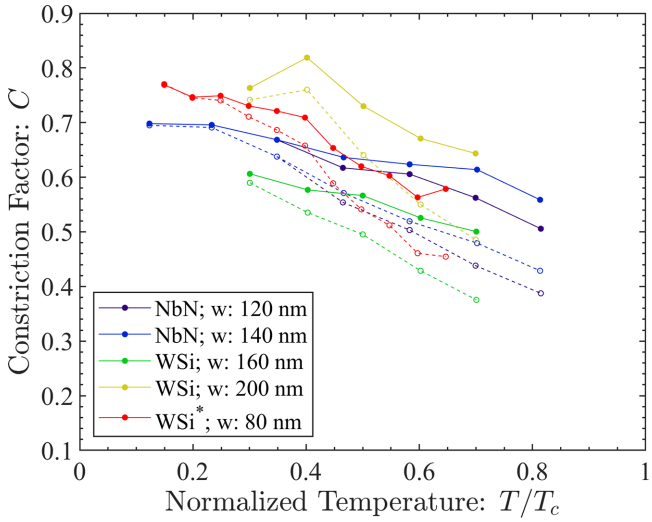

FIG. 4. Comparison of the extracted constriction factor for NbN and WSi nanowires using the CK fast relaxation model (dashed) and the temperature oscillation enhanced model (solid). Results are shown for a selection of NbN and WSi samples from Frasca *et al.* [4] and the 80-nm-wide WSi* device from Colangelo *et al.* [1]. The trends are qualitatively the same as previously extracted, but the magnitude of the decrease in constriction factor with increasing temperature is smaller than initially estimated.

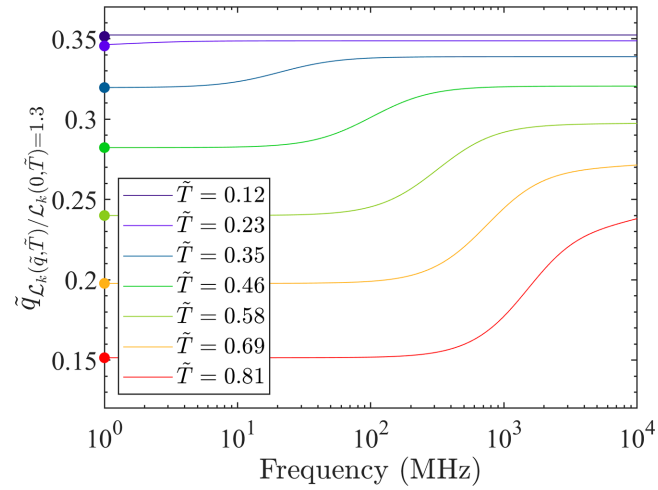

FIG. 5. Frequency dependence of the kinetic inductance shift with bias current as measured by the supermomentum q where the kinetic inductance increases by 30% compared to the zero current value. The results are shown for the NbN material parameters of Ref. [4]. The filled circles indicate the predictions of the CK fast relaxation model while the lines show the predictions of the temperature oscillation enhanced model.

ture resonator measurements shed light on the nature of the edge properties of superconducting nanowires, appropriately accounting for temperature oscillations when extracting the shift in kinetic inductance modeling will be necessary.

While our refined model of the kinetic inductance for dirty superconductors provides a marked improvement over the CK model, there are still deviations which occur. Part of this is expected to be measurement noise and the associated errors in the extracted kinetic inductance as a function of temperature and bias current. The lateral proximity effect may contribute to the remaining deviations, but this is expected to have minimal impact for nanowires with widths much larger than the twice coherence length. This is why we focused on the widest nanowires studied in Refs. [1,4] for our analysis. There is also uncertainty in the material parameters (τ_0, γ, and τ_{esc}), which could contribute to the residual error between theory and experiment. However, analysis of the experimental data using a range of these parameters shows that the formulation is largely insensitive to their exact values, so this is unlikely to be a dominant source of error, as demonstrated in Appendix C. Residual error might also be caused by only partial thermalization of the electron and phonon systems. Finally, at lower temperatures the validity of the two-temperature model, used for simplicity, may also become questionable.

B. Implications for resonator experiments

The uncertainty in the material parameters (τ_0, γ, and τ_{esc}) can increase the potential error in the measured depairing current. Partial thermalization of the electron and phonon systems can also increase the error of using this method by violating one of the core assumptions of the temperature oscillation model. Therefore, it is advantageous to understand the regimes where the temperature oscillation model can be simplified to the CK fast relaxation model to determine how future experiments should be performed in order to achieve optimal results. Intuitively, reducing the test frequency ω can bring the system to an operating point where the energy of Joule heating can dissipate through the phonon system to the substrate, leaving the electron and phonon temperatures at T_{sub}, which satisfies the condition of the CK fast relaxation model. Using our final result (31), we can estimate the frequency dependence of the shift in kinetic inductance with bias current in order to understand the operating regimes where the CK model can be used. To do this requires selecting a criterion for evaluating the shift in kinetic inductance. For convenience, we choose this metric to be the value of the $\tilde{q}$ such that the shift in $\mathcal{L}_k(\tilde{q},\tilde{T})$ compared to $\mathcal{L}_k(\tilde{q}=0,\tilde{T})$ is equal to 1.3. The value of 1.3 was chosen to approximately match the maximum shift in kinetic inductance observed in Ref. [4], but its precise value has little impact on the frequency dependence of the results. Defining this value as $\tilde{q}_{\mathcal{L}_k(\tilde{q},\tilde{T})/\mathcal{L}_k(0,\tilde{T})=1.3}$, in Fig. 5 we plot the result as a function for frequency for the material parameters of the NbN devices studied in Ref. [4] at the temperatures used to probe that device. The CK fast relaxation model results are indicated by the solid circles at a frequency of 1 MHz. For temperatures $\tilde{T} \geqslant 0.35$, there is a clear region where the response transitions from the CK fast relaxation model at lower frequencies to a higher value of $\tilde{q}$ at higher frequencies. This transition occurs in the tens of megahertz at lower temperatures up to the gigahertz range upon approach to T_c.

The implication of this result is that operating a resonator in a regime where the CK fast relaxation model applies for all temperature would require designing a device with a resonant frequency around 10 MHz. The problem with this approach is that decreasing the resonant frequency for a given resonator design requires fabricating proportionally longer

devices, which increases the likelihood of constrictions which reduce the switching current. The reduced switching current restricts the range of depairing current fraction which can be experimentally probed, and this increases the uncertainty and error in the extracted I_d. While fabricating such a long device seems infeasible, Fig. 5 shows that operating a device in the low hundreds of megahertz could provide a test of the regime where temperature oscillations can be neglected near T_c with a transition to the temperature oscillation regime around $\sim T_c/2$. Such an experiment would be a valuable test of the applicability of the temperature oscillation enhanced CK fast relaxation model.

V. CONCLUSION

The distribution of excited quasiparticles in a superconducting thin film must inevitably shift in response to an external alternating electric field due to Joule heating. When the driving frequency is sufficiently low that these excitations have time to thermalize, this response can be characterized by oscillations in the electron temperature of the system. By accounting for these temperature oscillations, we derive a revised form for the shift in kinetic inductance as a function of bias current and use this to extract the depairing current for recent experiments on NbN and WSi nanowires [1,4]. Compared to previous methods, our approach provides a substantially improved agreement between the theoretical and experimentally derived temperature dependence of the depairing current for these thin-film dirty superconductors. Our refinement to the Clem and Kogan model [5] is necessary to accurately extract the constriction factor from experimental measurements and evaluate the quality of nanofabrication techniques. It may also prove useful in the proper design of microwave superconducting circuits where DC bias-based shifts in kinetic impedance are used as a frequency tuning tool.

ACKNOWLEDGMENTS

Support for this work was provided in part by the Defense Advanced Research Projects Agency (DARPA) Defense Sciences Office (DSO) through the DETECT and Invisible Headlights programs. This work was carried out in part at the Jet Propulsion Laboratory, California Institute of Technology under a contract with the National Aeronautics and Space Administration (Contract No. 80NM0018D0004). The authors thank Stewart Koppel and Dip Joti Paul for feedback in preparing the final manuscript.

APPENDIX A: MODIFICATION OF THE CLEM AND KOGAN MODEL: IMPLICATIONS OF GENERALIZED TDGL

Clem and Kogan derived the kinetic impedivity following the standard TDGL model. It is worth analyzing the trends of the fits while allowing $\tau_{\rm eff}$ to change, i.e., replacing $\tau_{\rm eff}$ by $\tilde{\tau}_{\rm eff} = \tau_{\rm eff}\varrho(q,T)$, where we incorporate the dependence on both the bias current and the temperature. $\tilde{\tau}_{\rm eff}$ occurs in the generalized TDGL equations [14,15] and can be written in the form above with

$$\varrho(q,T) = \sqrt{1 + 4|\Delta(q,T)|^2\tau_{sc}(T)^2/\hbar^2}, \qquad \text{(A1)}$$

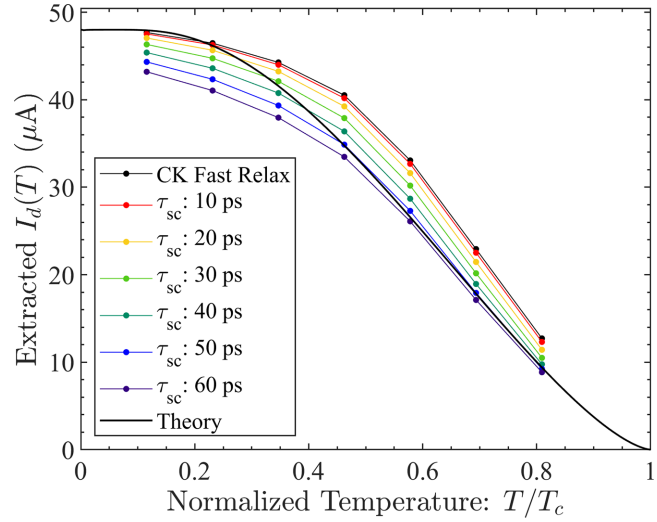

FIG. 6. Comparison of the generalized TDGL CK model with temperature-independent scattering times τ_{sc} ranging from 0 ps (CK slow experiment/fast relaxation) to 60 ps for a 140-nm-wide NbN nanowire [4]. The theory curve uses $I_d(0) = 48.0\,\mu$A, which is obtained by extrapolating the experimental results using the CK fast relaxation model to $T = 0$.

where $\tau_{sc}(T)$ is the inelastic scattering time for electrons and $\Delta(q,T)$ is the order parameter with the q dependence explicitly highlighted. The validity of generalized TDGL theory is the requirement $\omega, Dk^2 \ll \tau_{sc}^{-1}$, i.e., variations in space and time are slow [15], which is fulfilled for the experiments that we discuss. Figure 6 shows the extracted $I_d(T)$ for the 140-nm-wide NbN nanowire using the generalized TDGL model for different fixed $\tau_{sc}(T)$ in the range of 0 – 60 ps.

The expected dependence for both factors $\Delta(q,T)$ and τ_{sc} under the square root in (A1) is to decrease with increasing temperature. Therefore, a more realistic expectation would be a curve starting at the black fast relaxation curve near T_c and gradually moving closer to the colored curves with decreasing T depending on the actual magnitude of $\tau_{sc}(T)$. This behavior is distinctively different from the theoretical critical depairing current. Using $\tilde{\tau}_{\rm eff}(T)$ as a free fitting parameter in (8) one can obtain a nearly perfect fit for $I_d(T)$ in order to observe what trends in $\tilde{\tau}_{\rm eff}(T)$ are needed to match this model with experiment. The best fit $\tilde{\tau}_{\rm eff}(T)$, $\tau_s(T)$ and the required $\tau_{sc}(T)$ are shown in Fig. 7. The main feature is that the required $\tau_{sc}(T)$ must increase with T as shown by the red curve. Scaling the zero temperature depairing current [$(I_d(0)$] does alter the temperature dependence of the extracted scattering times, but unreasonably large decreases in $I_d(0)$ are needed to achieve a $\tau_{sc}(T)$ that decreases monotonically with increasing temperature. It is hard to think of any physical mechanism by which τ_{sc} would exhibit this behavior at these low temperatures apart from some resonant scattering. Moreover it is unlikely that this scattering is present in both NbN and WSi. Also if we include a comparison between the magnitudes of the required best fit τ_{sc} and the expected τ_{sc} at $T \simeq T_c$ we find the fitted value of τ_{sc} is significantly larger than expected. Summarizing, the use of both the standard and the generalized TDGL under the framework of the CK model of kinetic impedivity

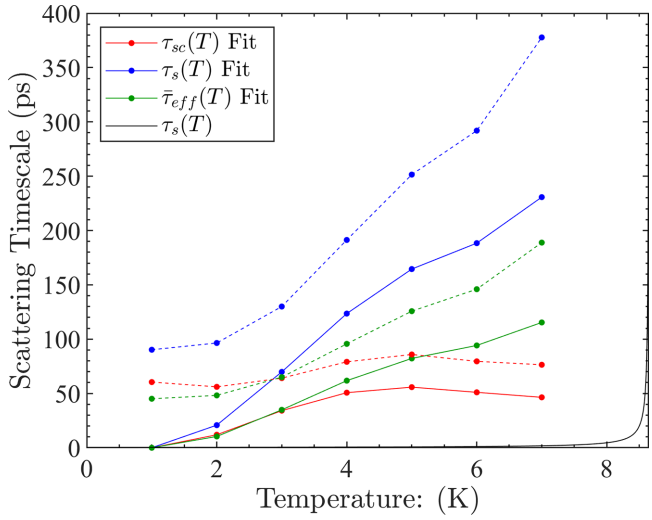

FIG. 7. Scattering timescales required to fit the extracted $I_d(T)$ to the theoretical temperature dependence for the 140-nm NbN sample of Ref. [4]. Symbols with solid lines correspond to $I_d(0) = 48.0\,\mu\text{A}$ while the symbols with dashed lines correspond to $I_d(0)$ scaled by 0.9. The solid black line shows τ_s as given by Eq. (3).

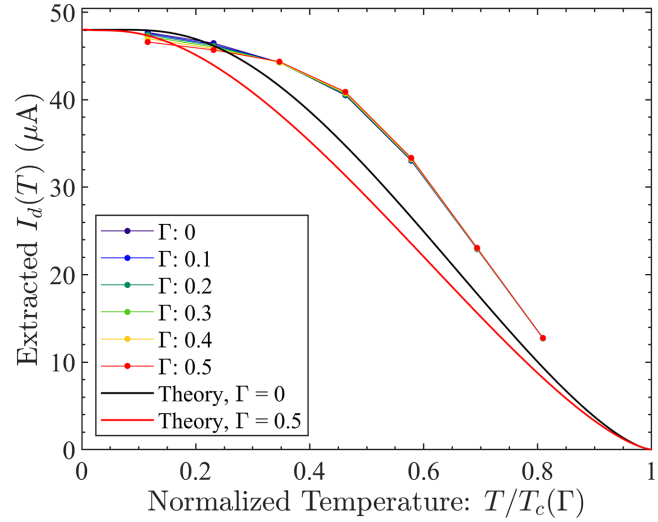

FIG. 8. Comparison of the impact of the scattering parameter Γ on the extracted $I_d(T)$ for the 140-nm-wide NbN results from [4]. The numerical solutions of the Usadel equations for $\Gamma = 0$ (black) and $\Gamma = 0.5$ with the depairing current at $T = 0$ normalized to $48.0\,\mu\text{A}$ are shown to compare the impact of Γ on the shape of the $I_d(T)$ curve. The value $\Gamma = 0.5$ corresponds to $T_{c,\text{matrix}} = 15.1\,\text{K}$. The value of $I_d(T = 0, \Gamma = 0.5)$ has been scaled to $48.0\,\mu\text{A}$ to compare the shape of the curve $I_d(T, \Gamma = 0.5)$ to $I_d(T, \Gamma = 0)$.

fail to reproduce the theoretical temperature dependence of critical depairing current of superconducting nanowires.

APPENDIX B: MODIFICATION OF THE CLEM AND KOGAN MODEL: MAGNETIC IMPURITIES/EXTRA PAIR-BREAKER EFFECT

One of the questions that requires special analysis to answer is the effect of extra pair breakers, such as paramagnetic impurities, on kinetic inductance. This can be done using the Abrikosov-Gor'kov theory [16] along the general lines suggested by Clem and Kogan by combining the supercurrent-induced depairing rate, $Q = \frac{1}{2}Dq^2$, and the depairing rate due to magnetic impurity scattering, Γ. By summing these contributions we proceed with the calculation of the change in kinetic inductance with bias current and temperature. To determine whether additional pair breaking might be responsible for the apparent deviation between experiment and theory, we calculate the normalized shift in kinetic inductance $\mathcal{L}_k(q, T, \Gamma)/\mathcal{L}_k(0, T, \Gamma)$ with different values of the parameter Γ and $T_{c,\text{matrix}}$. The meaning of the parameter $T_{c,\text{matrix}}$ is that we assume that the film may contain an undetected number of pair breakers such that the measured critical temperature corresponds to a certain pair-breaking rate, described by Γ, bringing $T_{c,\text{matrix}}$ down to the zero current $T_c(q = 0)$, which matches experiment. In this terminology, $T_{c,\text{matrix}}$ represents the critical temperature of the material if there were no extra pair breakers, i.e., $\Gamma = 0$. By fitting the resulting kinetic inductance shift to experimental results, the temperature dependence of the extracted depairing current can be compared to theory for different values of pair breaking.

Figure 8 shows the extracted depairing current with temperature for different values of the parameter Γ and $T_{c,\text{matrix}}$ which correspond to a T_c of 8.65 K for the 140 nm wide NbN device. There is very little shift in the shape of this extracted temperature dependence of the depairing current when accounting for pair-breakers. Moreover, the difference between the extracted dependencies and theoretical curves normalized to the same zero temperature critical depairing current increases with Γ. Thus, the transformation of the curves with increasing Γ is in the wrong direction, which apparently excludes extra pair-breakers as the source of the observed 'anomalous' behavior.

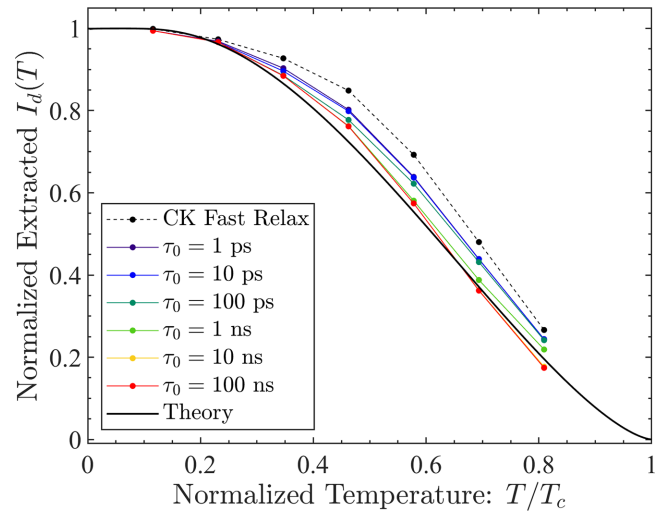

FIG. 9. Comparison of the extracted $I_d(T)$ using the temperature oscillation enhanced CK slow experiment/fast relaxation model for the 140-nm NbN sample of Ref. [4] for a range of values for the electron-phonon coupling timescale τ_0.

APPENDIX C: SENSITIVITY TO MATERIAL PARAMETERS

Due to the uncertainty in the material parameters used to extract the depairing current through the temperature oscillation enhanced kinetic inductance formulation (31), it is worth repeating the fitting using a range of material parameters in order to determine the sensitivity. We focus on the 140-nm-wide NbN sample from Ref. [4]. Figure 9 shows the extracted depairing current with temperature for a range of τ_0 with $T_c = 8.65\,\mathrm{K}$, $\tau_{\mathrm{esc}} = 20\,\mathrm{ps}$, and $\gamma = 20$. In the limit of $\omega\tau_2 \ll 1$, the results converge, but do not match the CK fast relaxation model due to the presence of oscillations in the phonon temperature. For $\tau_0 \geqslant 10\,\mathrm{ns}$, the curves converge, as there is no appreciable coupling between the electron and phonon systems. In the intermediate range there is a transition between these two extremes, with the transition occurring at different values of τ_0 for different temperatures. At larger temperatures, the transition occurs at longer timescales while at lower temperatures, the transition occurs for smaller values of τ_0. The phonon escape time τ_{esc} and phonon heat capacity parameter γ have an even smaller impact on the extracted depairing current once τ_0 is constrained to a reasonable range of values. Each of these parameters has only a small impact at the highest temperatures, $T/T_c > 0.6$, because that is the regime where the electron system is well thermalized with the phonon system so changes in the phonon system response become relevant. No combination of material parameters $(\tau_0, \gamma, \tau_{\mathrm{esc}})$ is able to completely reconcile the experimentally extracted depairing current with the theoretical temperature dependence in the temperature range of $0.3 < T/T_c < 0.6$. Only by assuming a 5% increase in the true T_c compared to the measured T_c is it possible to achieve a near-exact fit over the entire temperature range measured in experiment, but this is larger than the uncertainty of the T_c measurement and is not interpreted as an indication of measurement error.

[1] M. Colangelo, A. B. Walter, B. A. Korzh, E. Schmidt, B. Bumble, A. E. Lita, A. D. Beyer, J. P. Allmaras, R. M. Briggs, A. G. Kozorezov, E. E. Wollman, M. D. Shaw, and K. K. Berggren, Large-area superconducting nanowire single-photon detectors for operation at wavelengths up to 7.4 μm, Nano Lett. **22**, 5667 (2022).

[2] L. Zhang, L. You, D. Liu, W. Zhang, L. Zhang, X. Liu, J. Wu, Y. He, C. Lv, Z. Wang, and X. Xie, Characterization of superconducting nanowire single-photon detector with artificial constrictions, AIP Adv. **4**, 067114 (2014).

[3] F. Marsili, F. Najafi, E. Dauler, F. Bellei, X. Hu, M. Csete, R. J. Molnar, and K. K. Berggren, Single-photon detectors based on ultranarrow superconducting nanowires, Nano Lett. **11**, 2048 (2011).

[4] S. Frasca, B. Korzh, M. Colangelo, D. Zhu, A. E. Lita, J. P. Allmaras, E. E. Wollman, V. B. Verma, A. E. Dane, E. Ramirez, A. D. Beyer, S. W. Nam, A. G. Kozorezov, M. D. Shaw, and K. K. Berggren, Determining the depairing current in superconducting nanowire single-photon detectors, Phys. Rev. B **100**, 054520 (2019).

[5] J. R. Clem and V. G. Kogan, Kinetic impedance and depairing in thin and narrow superconducting films, Phys. Rev. B **86**, 174521 (2012).

[6] S. B. Kaplan, C. C. Chi, D. N. Langenberg, J. J. Chang, S. Jafarey, and D. J. Scalapino, Quasiparticle and phonon lifetimes in superconductors, Phys. Rev. B **14**, 4854 (1976).

[7] S. Anlage, H. Snortland, and M. Beasley, A current controlled variable delay superconducting transmission line, IEEE Trans. Magn. **25**, 1388 (1989).

[8] M. Tinkham, *Introduction to Superconductivity*, 2nd ed. (Dover, New York, 2004).

[9] M. Y. Kupriyanov and V. F. Lukichev, Temperature dependence of pair-breaking current in superconductors, Fiz. Nizk. Temp. **6**, 445 (1980) [Sov. J. Low Temp. Phys. **6**, 210 (1980)].

[10] D. Y. Vodolazov, Single-Photon Detection by a Dirty Current-Carrying Superconducting Strip Based on the Kinetic-Equation Approach, Phys. Rev. Appl. **7**, 034014 (2017).

[11] J. P. Allmaras, A. G. Kozorezov, B. A. Korzh, K. K. Berggren, and M. D. Shaw, Intrinsic Timing Jitter and Latency in Superconducting Nanowire Single-photon Detectors, Phys. Rev. Appl. **11**, 034062 (2019).

[12] D. Y. Vodolazov, Minimal Timing Jitter in Superconducting Nanowire Single-Photon Detectors, Phys. Rev. Appl. **11**, 014016 (2019).

[13] B. Korzh, Q.-Y. Zhao, J. P. Allmaras, S. Frasca, T. M. Autry, E. A. Bersin, A. D. Beyer, R. M. Briggs, B. Bumble, M. Colangelo, G. M. Crouch, A. E. Dane, T. Gerrits, A. E. Lita, F. Marsili, G. Moody, C. Peña, E. Ramirez, J. D. Rezac, N Sinclair *et al.*, Demonstration of sub-3 ps temporal resolution with a superconducting nanowire single-photon detector, Nat. Photonics **14**, 250 (2020).

[14] R. J. Watts-Tobin, Y. Krähenbühl, and L. Kramer, Nonequilibrium theory of dirty, current-carrying superconductors: phase-slip oscillators in narrow filaments near T_c, J. Low Temp. Phys. **42**, 459 (1981).

[15] N. B. Kopnin, *Theory of Nonequilibrium Superconductivity* (Oxford University Press, Oxford, 2001).

[16] A. A. Abrikosov and L. P. Gor'kov, Contribution to the theory of superconducting alloys with paramagnetic impurities, Z. Eksp. Teor. Fiz. **39**, 1782 (1960).

[17] See Supplemental Material at http://link.aps.org/supplemental/10.1103/PhysRevB.107.104520 for the discussion and calculation of electron-electron interaction times in dirty superconductors and discussion of the implications of edge defects on resonator depairing current measurements, which includes Refs. [20–28].

[18] I. Charaev, T. Silbernagel, B. Bachowsky, A. Kuzmin, S. Doerner, K. Ilin, A. Semenov, D. Roditchev, D. Y. Vodolazov, and M. Siegel, Proximity effect model of ultranarrow NbN strips, Phys. Rev. B **96**, 184517 (2017).

[19] Q. Chen, B. Zhang, L.-b. Zhang, F.-y. Li, F.-f. Jin, H. Han, R. Ge, G.-l. He, H.-c. Li, J.-r. Tan, X.-h. Wang, H. Wang, S.-l. Yu, X.-q. Jia, Q.-y. Zhao, X.-c. Tu, L. Kang, J. Chen, and P.-h. Wu, Suppression of superconductivity dominated by proximity effect in amorphous MoSi nanobelts, Phys. Rev. B **105**, 014516 (2022).

[20] X. Zhang, A. Engel, Q. Wang, A. Schilling, A. Semenov, M. Sidorova, H.-W. Hübers, I. Charaev, K. Ilin, and M. Siegel, Characteristics of superconducting tungsten silicide W_xSi_{1-x} for single photon detection, Phys. Rev. B **94**, 174509 (2016).

[21] X. Zhang, A. E. Lita, M. Sidorova, V. B. Verma, Q. Wang, S. W. Nam, A. Semenov, and A. Schilling, Superconducting fluctuations and characteristic time scales in amorphous WSi, Phys. Rev. B **97**, 174502 (2018).

[22] M. Sidorova, A. Semenov, H.-W. Hübers, K. Ilin, M. Siegel, I. Charaev, M. Moshkova, N. Kaurova, G. N. Goltsman, X. Zhang, and A. Schilling, Electron energy relaxation in disordered superconducting NbN films, Phys. Rev. B **102**, 054501 (2020).

[23] B. L. Altshuler and A. G. Aronov, in *Electron-Electron Interactions in Disordered Systems*, edited by A. L. Efros and M. Pollak (Elsevier Science, Amsterdam, 1985).

[24] A. Kamenev and A. Andreev, Electron-electron interactions in disordered metals: Keldysh formalism, Phys. Rev. B **60**, 2218 (1999).

[25] G. Eliashberg, Inelastic electron collisions and nonequilibrium stationary states in superconductors, Zh. Eksp. Teor. Fiz. **61**, 1254 (1971) [Sov. Phys. JETP **34**, 668 (1972)].

[26] M. Gulyan and G. F. Zharkov, Electron and phonon kinetics in a nonequilibrium Josephson junction, Zh. Eksp. Teor. Fiz. **89**, 156 (1985) [Sov. Phys. JETP **62**, 89 (1985)].

[27] J. Rammer and H. Smith, Quantum field-theoretical methods in transport theory of metals, Rev. Mod. Phys. **58**, 323 (1986).

[28] A. G. Aronov, Y. M. Gal'perin, V. L. Gurevich, and V. I. Kozub, The Boltzmann-equation description of transport in superconductors, Adv. Phys. **30**, 539 (1981).